Quantum and classical solutions for statically screened two-dimensional Wannier-Mott excitons

Adam J. Makowski*

Institute of Physics, Nicolaus Copernicus University, ul. Grudziądzka 5, PL-87100 Toruń, Poland

(Received 10 March 2011; revised manuscript received 23 May 2011; published 16 August 2011)

Quantum solutions and classical orbits are discussed for statically screened Wannier-Mott excitons for two closely related potentials: the Stern-Howard potential and a suggested simple focusing one. Bound states and exact "quantized" values of screening are obtained as well. For the suggested potential, the scattering matrix, the Regge poles, and the transmission coefficient are calculated exactly. We argue that the simple potential can be utilized in applications instead of the Stern-Howard potential, which is difficult to handle.

DOI: 10.1103/PhysRevA.84.022108 PACS number(s): 03.65.Ge, 71.35.−y

I. INTRODUCTION

Studying the electron-hole bound states known as excitons has a long history [1] in solid-state physics. Objects of this kind, with binding energy of the order of a few hundredths of eV and with radii of tens of angstroms, are called the Wannier-Mott excitons [2,3]. Since their radii are larger than the lattice spacings, the influence of the lattice on the excitons can be included in the effective mass of the electron-hole pair. The excitons are typically observed in semiconductor crystals with high dielectric constants, e.g., in Ge, Si, GaAs, CuO, and the like, and also in the liquid xenon. The literature on the subject is very rich, and we shall only mention here a few papers concerning calculations of the excitons' binding energies. One of the most common methods of describing the influence of electrons in the vicinity of an exciton on its spectrum is given in Ref. [4]. Of practical value is a simple method of calculating excitonic binding energies based on the model of fractional-dimensional space [5]. This method leads to a satisfactory agreement with the results obtained from an exact numerical procedure [6]. In another approach [7], the Bethe-Salpeter equation is used for the same purpose. In a recent study [8], the Monte Carlo method was proposed for studying changes in the character of an exciton during its propagation.

The interaction between an electron and a hole occurs through the Coulomb potential $-e^2/(\varepsilon r)$ and depends on the material in question via the value of the dielectric constant ε. In a semiconductor very often many electrons and holes are excited, and as a consequence, the Coulomb interaction of an electron-hole pair may be weakened. This leads to the phenomenon known as screening, usually modeled with the Stern-Howard potential [9]. Contemporary semiconductor growth techniques [10] are able to create high-quality two-dimensional (2D) systems where electrons and holes are restricted to move on a plane. Therefore, we are justified to use 2D theory, which, as observed in [11–15], leads, for the threshold energy $E = 0$, to an intriguing expression for quantization of the screening length. That result has never been formally derived, and no numerical estimates were made in order to evaluate its accuracy. The present paper contributes to the discussion of that problem, among other things.

*amak@fizyka.umk.pl

This paper is organized as follows. In Sec. II we study numerically the values of screening for which the Stern-Howard potential has excitonic bound states at the threshold energy and compare them with those obtained for a very simple focusing potential. For the latter potential it is possible to calculate exactly the scattering matrix and to find from its poles the quantization rule for screening. Moreover, we consider also the Regge poles and the transmission coefficient. In Sec. III classical solutions to both potentials are derived and compared to each other. Conclusions are given in Sec. IV.

II. QUANTUM SOLUTIONS

One of the most popular 2D statically screened potentials for the hydrogen-atom-like Wannier-Mott excitons [16–20] is given by the so-called Stern-Howard model [9]:

$$V_{SH}(r) = \frac{-e^2}{\varepsilon}\left\{\frac{1}{r} - \frac{\pi}{2} q[\mathbf{H_0}(qr) - N_0(qr)]\right\}. \tag{1}$$

Here ε is the dielectric constant, q [m^{-1}] is a screening parameter, $r = (\tilde{X}^2 + \tilde{Y}^2)^{1/2}$, and $\mathbf{H_0}$ and N_0 are the Struve and Neumann (the Bessel function of the second kind Y_0) functions, respectively. The radial part of the Schrödinger equation for $E = 0$,

$$\left[\frac{-\hbar^2}{2\mu^*}\left(\frac{d^2}{dr^2} + \frac{1}{r}\frac{d}{dr} - \frac{l^2}{r^2}\right) + V_{SH}(r)\right] R(r) = 0, \tag{2}$$

can be written in dimensionless quantities. To this end, we shall express all lengths in the effective Bohr radius a^* and energies in the effective Rydbergs $\mathcal{R}^*$:

$$a^* = \frac{\varepsilon\hbar^2}{\mu^* e^2}, \quad \mathcal{R}^* = \frac{e^2}{2\varepsilon a^*}. \tag{3}$$

In this way, we will get

$$\left[\frac{d^2}{d\rho^2} + \frac{1}{\rho}\frac{d}{d\rho} - \frac{l^2}{\rho^2} - V^*_{SH}(\rho)\right] R(\rho) = 0, \tag{4}$$

where

$$V^*_{SH}(\rho) = \frac{-2}{\rho}\left\{1 - q_s\rho\frac{\pi}{2}[\mathbf{H_0}(q_s\rho) - N_0(q_s\rho)]\right\}, \tag{5}$$

with

$$\rho = r/a^*, \quad q_s = qa^*. \tag{6}$$

For further discussion we shall also write

$$\frac{d^2R}{dx^2}+\frac{1}{x}\frac{dR}{dx}-\frac{l^2}{x^2}R + \frac{\lambda_{SH}}{x}\left\{1-\frac{\pi}{2}x[\mathbf{H_0}(x)-N_0(x)]\right\}R(x)=0, \quad (7)$$

where

$$x = q_s\rho = qr, \quad \lambda_{SH} = 2/q_s. \quad (8)$$

In close relation to the potential in Eq. (1), there is the following one:

$$V_{1/2}(r) = \frac{-e^2}{\varepsilon r(1+qr)^2}, \quad (9)$$

which is a member of a large family of focusing Lenz-Demkov-Ostrovsky potentials [21–23]. The potentials in Eqs. (1) and (9) have exactly the same limiting behavior at small $-e^2/(\varepsilon r)$ and at large distances $-e^2/(\varepsilon q^2 r^3)$. In between the two limits, the differences between them are quite small, as discussed in detail in [24]. Now, using the same notation as in Eq. (7), we obtain

$$\frac{d^2R}{dx^2}+\frac{1}{x}\frac{dR}{dx}-\frac{l^2}{x^2}R+\frac{\lambda_{1/2}}{x(1+x)^2}R(x)=0, \quad \lambda_{1/2}=2/q_s. \quad (10)$$

A. Bound states

Equation (10) has normalized solutions provided that the screening length $\lambda_{1/2}$ is "quantized" according to the rule [24,25]

$$\lambda_{1/2} = (n+2l)(n+2l+1), \quad (11)$$

with l and n denoting the angular momentum quantum number and the number of nodes of the corresponding wave functions, respectively. As shown in [24], the exact functions can be written in terms of the Gegenbauer polynomials C_n^σ:

$$R_{nl}(x) = N_{nl}\frac{x^l}{(1+x)^{2l}}C_n^{2l+1/2}\left(\frac{1-x}{1+x}\right), \quad (12)$$

where the normalization factor N_{nl} is derived in Appendix A.

If integer and half-integer angular momenta are accepted, then the number of degenerate bound states $R_{nl}(x)$, corresponding to a given $\lambda_{1/2}$, is equal to $Q = n + 2l - 2$. For instance, when $\lambda_{1/2} = 12$, there is only one normalizable state $(n,l) = (0,3/2)$. When, e.g., $\lambda_{1/2} = 72$, we have six states: $(n,l) = (0,4),(1,7/2),(2,3),(3,5/2),(4,2),(5,3/2)$ and so on.

Some time ago [11] the right-hand side of Eq. (11) was proposed as a proper quantization rule for the screening length λ_{SH} for the Stern-Howard potential, and later it was considered to be a not strictly exact result [25]. We have shown in a recent paper [24] that the values of λ_{SH} have to be different from those for $\lambda_{1/2}$ to have solutions of Eq. (7) with a correct asymptotic behavior and hence representing bound states.

Since no exact analytical solutions seem to be possible for Eq. (7), we integrated the equation numerically and obtained the allowable values of λ_{SH} for which the solutions represent bound states. Results are given in Tables I and II for integer and half-integer angular momenta, respectively. Now, there is no degeneracy, and differences between the values of λ_{SH} and the corresponding single $\lambda_{1/2}$ are not large and are very slowly growing with increasing values of the quantum numbers n and l. The number of bound states is still equal to Q defined above if we consider now the states grouping near a selected value of $\lambda_{1/2}$. We should emphasize at this point that neither of the potentials has bound states for $l = 0$ and $l = 1$. All this shows that the potentials in Eqs. (1) and (9) are, indeed, in close relation and that particular $\lambda_{1/2}$ are roughly the centers of the "bands" composed of the values of λ_{SH}. Nevertheless, the screening lengths λ_{SH} do not obey rule (11), which is exact exclusively for the potential in Eq. (9).

B. Scattering matrix

We shall now show two other ways of obtaining formula (11). In the first one, the quantization of screening will be a result of the square integrability of the solutions represented by hypergeometric functions. In the second way, we shall derive the scattering matrix and show the connection of its poles with discrete values of the screening. Next, it can be proved that for the quantized values of $\lambda_{1/2}$ in Eq. (11) the potential in Eq. (9) is completely transparent.

First, we will find solutions of Eq. (10) in a form suitable for S-matrix calculations. Changing the independent variable according to the relation $x = \exp(y)$, we get from Eq. (10)

$$\left(\frac{d^2}{dy^2}-l^2+\frac{\lambda_{1/2}\exp(y)}{[1+\exp(y)]^2}\right)R(y)=0, \quad (13)$$

which constitutes a 1D problem with the Eckart potential

$$\frac{\lambda_{1/2}\exp(y)}{[1+\exp(y)]^2} = \frac{\lambda_{1/2}}{4\cosh^2(y/2)}, \quad (14)$$

with l^2 playing the role of energy. Further, Eq. (13) can be transformed to a hypergeometric equation in the following steps. First, we take

$$z = \sinh^2(y/2) \quad (15)$$

and then look for the solution $R(z)$ in the form

$$R(z) = (1+z)^b f(z), \quad (16)$$

where

$$b = \tfrac{1}{4}(1-\sqrt{1+4\lambda_{1/2}}). \quad (17)$$

In this way, also changing z to $-z$, we have

$$z(1-z)\frac{d^2f}{dz^2}+(1/2-z-2bz)\frac{df}{dz}-(b^2-l^2)f=0. \quad (18)$$

This is a standard equation for the hypergeometric function $F(\alpha,\beta;\gamma;z)$ if

$$\alpha = b+l, \quad \beta = b-l, \quad \gamma = 1/2. \quad (19)$$

Two independent solutions of Eq. (18),

$$f_1(z) = A_1F(\alpha,\beta;\gamma;z), \quad (20)$$

$$f_2(z) = A_2z^{1-\gamma}F(\alpha-\gamma+1,\beta-\gamma+1;2-\gamma;z), \quad (21)$$

are finite for $z = 0 (y = 0)$. In order the wave function be square integrable, the hypergeometric functions have to reduce to polynomials. This is the case when

$$\alpha = \frac{1}{4}(1 - \sqrt{1+4\lambda_{1/2}}) + l = -n, \tag{22}$$

$$\alpha - \gamma + 1 = \frac{1}{4}(1 - \sqrt{1+4\lambda_{1/2}}) + l + \frac{1}{2} = -n, \tag{23}$$

with $n = 0,1,2,\ldots$. Thus, for the even $(2n)$ and odd $(2n+1)$ values, we get, respectively,

$$2n + 2l + \frac{1}{2} = \frac{1}{2}\sqrt{1+4\lambda_{1/2}}, \tag{24}$$

$$2n + 1 + 2l + \frac{1}{2} = \frac{1}{2}\sqrt{1+4\lambda_{1/2}}. \tag{25}$$

The two formulas can be reduced to the single formula

$$n + 2l + \frac{1}{2} = \frac{1}{2}\sqrt{1+4\lambda_{1/2}}, \tag{26}$$

which is valid for all natural n. Obviously, this equation leads at once to rule (11).

As the final step of this part of the calculations, we give the explicit expression for the wave functions. After using equations (15), (16), (19), (20), and (21), we can write

$$\begin{aligned} R(y) = {} & N_1[\cosh(y/2)]^{2b} F(b+l, b-l; 1/2; -\sinh^2(y/2)) \\ & + N_2[\cosh(y/2)]^{2b}\sinh(y/2) F(b+l \\ & + 1/2, b-l+1/2; 3/2; -\sinh^2(y/2)), \end{aligned} \tag{27}$$

where N_1 and N_2 are constants of integration. For bound states, Eq. (27) can be reduced to the simple form of the solution given in Eq. (12).

To find the scattering matrix and related quantities, we can utilize solution (27), in which we put $l \to il$. Since $y = \ln(x) = \ln(q_s\rho) = \ln(qr)$, therefore, if $0 \leqslant r < \infty$, then $-\infty < y < +\infty$. From asymptotic properties of the hypergeometric functions, we can obtain

$$R(y) \longrightarrow A\exp(ily) + B\exp(-ily), \quad y \to -\infty, \tag{28}$$

$$R(y) \longrightarrow C\exp(ily) + D\exp(-ily), \quad y \to +\infty, \tag{29}$$

where

$$\begin{aligned} A &= 4^{il}(N_1 u - N_2 v), \\ B &= 4^{-il}(N_1 u^* - N_2 v^*), \\ C &= 4^{-il}(N_1 u^* + N_2 v^*), \\ D &= 4^{il}(N_1 u + N_2 v), \end{aligned} \tag{30}$$

and

$$\begin{aligned} u &= \frac{\sqrt{\pi}\,\Gamma(-2il)}{\Gamma(b-il)\Gamma(-b+1/2-il)}, \\ v &= \frac{\sqrt{\pi}\,\Gamma(-2il)}{2\Gamma(b+1/2-il)\Gamma(-b+1-il)}. \end{aligned} \tag{31}$$

The scattering matrix S obeys the relation

$$\begin{bmatrix} C \\ B \end{bmatrix} = \begin{bmatrix} S_{11} & S_{12} \\ S_{21} & S_{22} \end{bmatrix} \begin{bmatrix} A \\ D \end{bmatrix},$$

and its components are given as

$$\begin{aligned} S_{11} &= S_{22} \\ &= \frac{i\sinh(2\pi l)\Gamma(2il)\Gamma(2b-2il)\Gamma(-2b+1-2il)}{\pi\Gamma(-2il)}, \end{aligned} \tag{32}$$

$$\begin{aligned} S_{12} &= S_{21} \\ &= \frac{\sin(2\pi b)\Gamma(2il)\Gamma(2b-2il)\Gamma(-2b+1-2il)}{\pi\Gamma(-2il)}. \end{aligned} \tag{33}$$

Putting now $l \to il$, we can see that the poles of the S matrix are in the points

$$\begin{aligned} -2b - 2l &= n \quad (= 0,1,2,\ldots), \\ -2b + 2l + 1 &= 0, -1, -2, \ldots, \\ 2l &= 0,1,2,\ldots. \end{aligned} \tag{34}$$

The first line of Eqs. (34), after using the definition of b in Eq. (17), gives again the exact formula for bound states in Eq. (11). The second equation leads to a discrepancy since $b < 0$ and $l > 1$. The third condition represents so-called false poles or extra poles.

As is well known, each bound state is associated with a pole of the S matrix, but the inverse statement is not always true. The potential $V_{1/2}$, for which we have derived the scattering matrix, is an example of this kind since the extra poles are not related to bound states. A separation of the extra poles from the physical ones is possible when the potential under consideration is truncated at some sufficiently large distance. A detailed discussion on the subject can be found in Ref. [26].

The position of Regge poles as a function of the screening parameter q_s can be easily found to be

$$l(q_s) = \frac{1}{2}\left(\sqrt{\frac{1}{4} + \frac{2}{q_s}} - n - \frac{1}{2}\right), \tag{35}$$

with the condition $l(q_s) > 0$ and $n = 0,1,2,\ldots$. This agrees with a similar result found in a different context in [27]. The number of Regge poles, in the right half plane, grows with the growing strength of the potential or with the decreasing screening q_s. For the repulsive $V_{1/2}$ potential, there are no Regge poles in the right half plane.

One can also calculate the transmission coefficient T for the considered potential at $E = 0$. From Eqs. (32) and (33), we get

$$\begin{aligned} T &= \frac{1}{1 + |\frac{S_{12}}{S_{11}}|^2} \\ &= \frac{\sinh^2(2\pi l)}{\sinh^2(2\pi l) + \cos^2(\frac{\pi}{2}\sqrt{1+4\lambda_{1/2}})}. \end{aligned} \tag{36}$$

The plot of T versus $\lambda_{1/2}$, for $l = 2$, is given in Fig. 1. The transmission coefficient has maxima, all equal to 1, if $\frac{\pi}{2}\sqrt{1+4\lambda_{1/2}} = (2k+1)\frac{\pi}{2}$, $k = 0,1,2,\ldots$, i.e., for $\lambda_{1/2} = k(k+1) = 0,2,6,12,20,30,42$, and so on. There are no bound states corresponding to the values of 0, 2, and 6. The next maximum, for $\lambda_{1/2} = 12$, is related to the bound state with $l = 3/2$ (see Table II). All remaining values for which we have

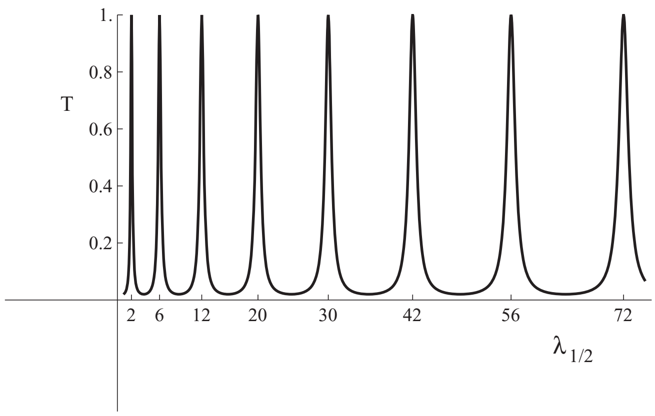

FIG. 1. Plot of the transmission coefficient T in Eq. (36) vs $\lambda_{1/2}$. To make the oscillations of T clearly visible, the amplitudes of the cosine fuction were multiplied by a factor of 10^{12}. As discussed in the text, the succeeding maxima correspond to the values of $\lambda_{1/2}$ in Eq. (11).

maxima correspond to the bound states with integer angular momenta (see Table I). So we can conclude that the attractive potential $V_{1/2}$ is totally transparent for some discrete values of screening. The same is expected for the Stern-Howard potential as well.

We should note at this point that for $\lambda_{1/2} = 2$ with $(n,l) = (0,1/2),(1,0)$ and for $\lambda_{1/2} = 6$ with $(n,l) = (0,1),(1,0),(1,1/2)$, the exact solutions in Eq. (12) are all finite everywhere in the interval $0 \leqslant x < \infty$, but they do not decay fast enough at infinity to be square integrable. They are called half-bound states or zero-energy resonances and correspond to the first two maxima in Fig. 1.

If $V_{1/2}$ is a repulsive potential, the transmission coefficient can also be found. It follows immediately from Eq. (36), where we have to replace $\lambda_{1/2}$ with $-\lambda_{1/2}$. Now, there are no oscillations in T, and the coefficient is a diminishing function of the coupling constant $\lambda_{1/2}$.

III. CLASSICAL SOLUTIONS

Classical equations of motion can also be integrated exactly for the potential $V_{1/2}(r)$, and the solution can be given in terms of integrals of motion: the total energy E and the angular momentum L. We can introduce the same system of units and notation as in the quantum case. To this end, it is enough to replace the classical angular momentum L with $\gamma\hbar$, where γ is a dimensionless scale factor. Then, using the polar coordinates $\tilde{X} = r\cos\varphi$ and $\tilde{Y} = r\sin\varphi$, we get for $V_{1/2}(r)$ and $E = 0$ in the 2D configuration space

$$\left(\frac{dx}{d\varphi}\right)^2 + x^2 = \frac{\lambda_c x^3}{(1+x)^2} = \frac{\lambda_c x^2}{\left(x^{-1/2} + x^{1/2}\right)^2}, \tag{37}$$

where $\lambda_c = 2/\tilde{q}_s = \lambda_{1/2}/\gamma^2$, $\tilde{q}_s = \gamma^2 q a^* = \gamma^2 q_s$, and $x = qr$. The equivalent form of Eq. (37) can be found as

$$\left[2\frac{d}{d\varphi}(x^{1/2} - x^{-1/2})\right]^2 + (x^{1/2} - x^{-1/2})^2 = \lambda_c - 4. \tag{38}$$

Now, the exact solution can be easily obtained, and we have

$$x^{1/2} - x^{-1/2} = \pm 2\{C_1 \sin[(\varphi - \varphi_0)/2] + C_2 \cos[(\varphi - \varphi_0)/2]\}, \tag{39}$$

where

$$C_1^2 + C_2^2 = \lambda_c/4 - 1 \tag{40}$$

and C_1 and C_2 are real constants of integration. They are determined by the relations $C_1 = \sqrt{\lambda_c/4 - 1 - C_2^2}$ and $C_2^2 = (1/4)(x_0^{1/2} - x_0^{-1/2})^2$, where x_0 is the initial position for an initial angle.

The solution $x = x(\varphi)$ from Eq. (39) is plotted in Fig. 2 (solid line) for $\lambda_{1/2} = 20$, $\gamma^2 = 2$, and $C_2 = 0$ from which $x_0 = 1$. As a result, we get the limacon of a Pascal-shaped curve. Using the same units, notation, and initial conditions, we integrated numerically the classical equations of the motion for the Stern-Howard potential as well. Again, a similarly shaped curve is obtained for $\lambda_{SH} = 20.022524$ (dashed line). The differences between the two curves follow from some differences between the potentials $V_{1/2}$ and V_{SH}. We have to note at this point that the orbits for V_{SH}, even for large values of λ_{SH}, are about the same in shape for each particular value of the screening length within a selected band. Thus the curves in

TABLE I. Values of λ_{SH} from Eq. (7) for which solutions of the equation are square integrable. For comparison, the first column contains the corresponding values of $\lambda_{1/2}$ from Eq. (11).

$\lambda_{1/2}$	$n+2l$	$l=2$	$l=3$	$l=4$	$l=5$	$l=6$	$l=7$
20	4	20.022 524					
30	5	29.959 704					
42	6	41.934 331	42.063 091				
56	7	55.933 377	55.961 382				
72	8	71.947 402	71.898 862	72.126 555			
90	9	89.970 287	89.866 892	89.984 127			
110	10	109.998 322	109.857 905	109.881 986	110.213 443		
132	11	132.029 357	131.865 822	131.813 870	132.029 325		
156	12	156.062 181	155.886 004	155.773 770	155.886 243	156.323 980	
182	13	182.096 128	181.915 026	181.756 340	181.779 380	182.097 603	
210	14	210.130 843	209.950 411	209.757 035	209.703 873	209.912 800	210.458 281
240	15	240.166 145	239.990 389	239.772 112	239.655 134	239.765 709	240.189 281

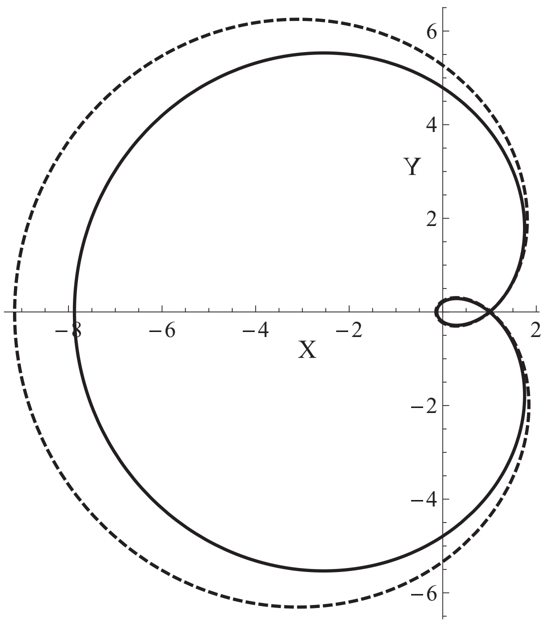

FIG. 2. Plots of the orbits $x = x(\varphi)$ for the potentials V_{SH} in Eq. (1) (dashed line) and $V_{1/2}$ in Eq. (9) (solid line), where $x = qr = q\sqrt{\tilde{X}^2 + \tilde{Y}^2}$ and $\varphi = \tan^{-1}(\tilde{Y}/\tilde{X})$. The labels X and Y denote, respectively, $X = q\tilde{X}$ and $Y = q\tilde{Y}$. The plots are in dimensionless units, as explained in the text.

Fig. 2 can be considered to be a characteristic image or simply an icon of the discussed model of the Wannier-Mott exciton.

IV. CONCLUSION

We have studied here the validity of formula (11) for the spectrum of allowed values of the screening lengths λ_{SH} for the Stern-Howard potential. This is important since the potential V_{SH} is one of the most popular models used for Wannier-Mott excitons. It is shown that the formula is not exact for the values of λ_{SH}; however, the numerically calculated "true" values shown in Tables I and II differ slightly from those obtained from Eq. (11). Then, why not use in applications the potential $V_{1/2}$ instead of V_{SH}? As we have shown in Secs. II and III, the former enables formally exact calculations for many quantities. Among them, we have obtained the S matrix, the Regge poles, and the transmission coefficient.

It is also interesting that $V_{1/2}(x) = -\lambda_{1/2}/[x(1+x)^2]$ belongs to the class of potentials expressible as a superposition of Yukawa potentials [27,28]

$$V_{1/2}(x) = -\lambda_{1/2}\int_0^\infty \frac{\exp(-\mu x)}{x}\exp(-\mu)\mu d\mu. \quad (41)$$

This is not the case for the Stern-Howard potential

$$V_{SH}(x) = \frac{-\lambda_{SH}}{x}\left\{1 - \frac{\pi}{2}x[\mathbf{H_0}(x) - N_0(x)]\right\}. \quad (42)$$

However, we can find for it an analog in the form

$$V_{SH}(x) = -\lambda_{SH}x\int_0^\infty \frac{\exp(-\mu x)}{x}\left(1 - \frac{1}{\sqrt{1+\mu^2}}\right)d\mu. \quad (43)$$

This representation follows from formula 2.3.5(6) in [29],

$$\int_0^\infty \frac{\exp(-\mu x)}{\sqrt{1+\mu^2}}d\mu = \frac{\pi}{2}x[\mathbf{H_0}(x) - N_0(x)]. \quad (44)$$

One more argument in favor of $V_{1/2}$ is the following: The physically important quantity, the ionization degree for a fixed q_s, depends on the sum over all angular momenta l. When the quasiclassical limit is utilized, then, for large l, the total number of bound states is given by the integral

$$\lambda = -\int_0^\infty xV(x)dx. \quad (45)$$

If $V(x) = V_{1/2}(x)$ [cf. Eq. (10)], we get at once $\lambda = \lambda_{1/2} = 2/q_s$, and its values are given in Eq. (11). If $V(x) = V_{SH}(x)$ [cf. Eq. (7)], the rhs of Eq. (45) is again equal to $\lambda = \lambda_{SH} = 2/q_s$ (see Appendix B), but the screening is not quantized according to rule (11). Now, the bound states are found to be as given in Tables I and II. The small differences in the values of λ do not affect the results for ionization degree in the low-density limit [13]. That is why we are allowed to use again the simple focusing potential $V_{1/2}$ instead of the difficult-to-handle Stern-Howard one.

We have also considered the classical solutions of both related potentials. Contrary to the quantum case, where bound states exist only for $\lambda_{1/2}$ and λ_{SH} being precisely as given

TABLE II. As in Table I but for the half-integer values of the angular momentum l.

$\lambda_{1/2}$	$n+2l$	$l=\frac{3}{2}$	$l=\frac{5}{2}$	$l=\frac{7}{2}$	$l=\frac{9}{2}$	$l=\frac{11}{2}$	$l=\frac{13}{2}$
12	3	12.010 441					
20	4	19.965 813					
30	5	29.957 321	30.040 002				
42	6	41.968 158	41.958 053				
56	7	55.988 261	55.914 531	56.091 918			
72	8	72.012 450	71.898 974	71.970 008			
90	9	90.038 346	89.902 882	89.887 893	90.167 053		
110	10	110.064 973	109.919 978	109.838 283	110.003 870		
132	11	132.091 987	131.945 882	131.814 446	131.881 382	132.265 747	
156	12	156.119 311	155.977 641	155.810 645	155.794 129	156.060 554	
182	13	182.146 972	182.013 311	181.822 225	181.736 720	181.896 688	182.388 155
210	14	210.175 038	210.051 624	209.845 521	209.704 200	209.769 853	210.140 503

in Tables I and II, the classical solutions are not sensitive to the exact values of λ. It is interesting that closed orbits corresponding to the bound states of both potentials are all of the limacon of Pascal shape.

Closed classical orbits are usually expected for potentials having bound states, as in the present paper. Nevertheless, there can be some singular potentials with square-integrable solutions at $E = 0$ where closed classical trajectories do not exist. Examples are given in Refs. [30,31].

ACKNOWLEDGMENTS

The values in Tables I and II were calculated with the help of the FORTRAN code written by Professor L. Wolniewicz (Institute of Physics, Nicolaus Copernicus University). The present work was inspired by the correspondence with Dr. M. E. Portnoi (School of Physics, University of Exeter, UK).

APPENDIX A

Normalization of the function $R_{nl}(x)$ in Eq. (12) in 2D space leads to the integral

$$q^2 = N_{nl}^2 \int_0^\infty x R_{nl}^2(x) dx. \tag{A1}$$

Performing the integral is not simple and can be done in the following steps. First, change the variable $\xi = (1-x)/(1+x)$ and then introduce a new one $\xi = -\eta$. Next, use the parity property [32]

$$C_n^\sigma(-\eta) = (-1)^n C_n^\sigma(\eta) \tag{A2}$$

of the Gegenbauer polynomials and the recurrence relation [33]

$$(n+2l+1/2)C_n^{2l+1/2}(\eta) = (2l+1/2)\left[C_n^{2l+3/2}(\eta) - C_{n-2}^{2l+3/2}(\eta)\right]. \tag{A3}$$

Thus, we will derive

$$q^2 = \frac{N_{nl}^2(2l+1/2)}{2^{4l-1}(n+2l+1/2)} \int_{-1}^1 (1+\eta)^{2l+1}(1-\eta)^{2l-3} C_n^{2l+1/2}(\eta) \times \left[C_n^{2l+3/2}(\eta) - C_{n-2}^{2l+3/2}(\eta)\right] d\eta. \tag{A4}$$

As a final step, we use formula 2.21.18(5) in Ref. [34]. In this way, we have, for $l > 1$,

$$\frac{q^2}{N_{nl}^2} = \frac{\left(2l+\frac{1}{2}\right)(4l+n)B(2l+2,2l-2)}{24n!n!l\left(n+2l+\frac{1}{2}\right)\Gamma(4l+3)} \times [f(n) - n(n-1)(4l+n-1) \times (4l+n-2)f(n-2)], \tag{A5}$$

where $B(a,b)$ is the beta function, and

$$f(\nu) = \Gamma(4+\nu)\Gamma(4l+3+\nu)\,{}_4F_3(-n,4l+1+n,2l-2,-3;2l+1,4l+\nu,-\nu-3;1), \tag{A6}$$

with ${}_4F_3$ denoting the generalized hypergeometric function. Thanks to the value of $\alpha_4 = -3$, the infinite series representing the function ${}_4F_3(\alpha_1,\alpha_2,\alpha_3,\alpha_4;\beta_1,\beta_2,\beta_3;1)$ terminates after four terms.

APPENDIX B

We shall prove here that λ in Eq. (45) is equal to λ_{SH} if $V(x) = V_{SH}(x)$. To this end, we insert formula (43) into Eq. (45) and integrate over x. This gives $1/\mu^2$, and hence, we have

$$\lambda = \lambda_{SH} \int_0^\infty \frac{1}{\mu^2}\left(1 - \frac{1}{\sqrt{1+\mu^2}}\right) d\mu = \lambda_{SH}\left(\frac{-1}{\mu} + \frac{\sqrt{1+\mu^2}}{\mu}\right)\Bigg|_0^\infty. \tag{B1}$$

Now, using the expansion

$$\sqrt{1+\mu^2} = 1 + \frac{1}{2}\mu^2 - \frac{1\cdot 1}{2\cdot 4}\mu^4 + \frac{1\cdot 1\cdot 3}{2\cdot 4\cdot 6}\mu^6 - \ldots, \tag{B2}$$

we finally get

$$\lambda = \lambda_{SH}\left[\lim_{\mu\to 0}\frac{1}{\mu} + 1 - \lim_{\mu\to 0}\frac{1}{\mu} - \lim_{\mu\to 0}\left(\frac{1}{2}\mu - \frac{1\cdot 1}{2\cdot 4}\mu^3 + \frac{1\cdot 1\cdot 3}{2\cdot 4\cdot 6}\mu^5 - \ldots\right)\right] = \lambda_{SH}. \tag{B3}$$

[1] *Excitons*, edited by E. I. Rashba and M. Sturge (North-Holland, Amsterdam, 1982).
[2] G. Wannier, Phys. Rev. **52**, 191 (1937).
[3] N. F. Mott, Trans. Faraday Soc. **34**, 500 (1938).
[4] L. Hedin, Phys. Rev. **139**, A796 (1965).
[5] H. Mathieu, P. Lefebvre, and P. Christol, Phys. Rev. B **46**, 4092 (1992).
[6] L. C. Andreani and A. Pasquarello, Phys. Rev. B **42**, 8928 (1990).
[7] F. Fuchs, C. Rödl, A. Schleife, and F. Bechstedt, Phys. Rev. B **78**, 085103 (2008).
[8] V. I. Sugakov and G. V. Vertsimakha, Phys. Rev. B **81**, 235308 (2010).
[9] F. Stern and W. E. Howard, Phys. Rev. **163**, 816 (1967).
[10] G. Cao and Y. Wang, *Nanostructures and Nanomaterials: Synthesis, Properties, and Applications* (World Scientific, Singapore, 2011), Chaps. 5 and 7.
[11] M. E. Portnoi and I. Galbraith, Solid State Commun. **103**, 325 (1997).
[12] M. E. Portnoi and I. Galbraith, Phys. Rev. B **58**, 3963 (1998).
[13] M. E. Portnoi and I. Galbraith, Phys. Rev. B **60**, 5570 (1999).
[14] D. G. W. Parfitt and M. E. Portnoi, e-print arXiv:cond-mat/0410095v1.
[15] D. G. W. Parfitt and M. E. Portnoi, Phys. E **17**, 212 (2003).

[16] N. BenBrahim Aouani, L. Mandhour, R. Bennaceur, S. Jasiri, T. Amand, and X. Marie, Solid State Commun. **108**, 199 (1998).
[17] H. N. Spector, J. Lee, and P. Melman, Superlattices Microstruct. **1**, 149 (1985).
[18] J. Lee, H. N. Spector, and P. Melman, J. Appl. Phys. **58**, 1893 (1985).
[19] W. S. Edelstein and H. N. Spector, Surf. Sci. **224**, 581 (1989).
[20] J. A. Reyes and M. del Castillo-Mussot, Phys. Rev. B **56**, 14893 (1997).
[21] W. Lenz, in *Probleme der Modernen Physik*, edited by P. Debye (Hirsel, Leipzig, 1928).
[22] Yu. N. Demkov and V. N. Ostrovsky, Zh. Eksp. Teor. Fiz. **60**, 2011 (1971) [Sov. Phys. JETP **33**, 1083 (1971)].
[23] Yu. N. Demkov and V. N. Ostrovsky, Zh. Eksp. Teor. Fiz. **62**, 125 (1972); **63**, 2376(E) (1972) [Sov. Phys. JETP **35**, 66 (1972)].
[24] A. J. Makowski, Phys. Rev. A **83**, 022104 (2011).
[25] C. Tanguy, e-print arXiv:cond-mat/0106184v1; e-print arXiv:cond-mat/0110464v1.
[26] A. G. Sitenko, *Scattering Theory* (Springer, Berlin, 1991), Chap. 7.5.
[27] H. Cheng, Nuovo Cimento A **45**, 487 (1966).
[28] C. J. Joachain, *Quantum Collision Theory* (North-Holland, Amsterdam, 1983), Chap. 11.4.
[29] A. P. Prudnikov, Yu. A. Brychkov, and O. I. Marichev, *Integrals and Series: Elementary Functions* (Fizmatlit, Moscow, 2002), Vol. I (in Russian).
[30] A. J. Makowski and K. J. Górska, Phys. Lett. A **362**, 26 (2007).
[31] A. J. Makowski and K. J. Górska, J. Phys. A **40**, 11373 (2007).
[32] H. Bateman and A. Erdélyi, *Higher Transcendental Functions* (McGraw-Hill, New York, 1953), Vol. II, Chap. 10.9.
[33] See Eq. (36) in Ref. [32].
[34] A. P. Prudnikov, Yu. A. Brychkov, and O. I. Marichev, *Integrals and Series: Special Functions* (Fizmatlit, Moscow, 2003), Vol. II (in Russian).